

# Bulk-edge Correspondence in the Adiabatic Heuristic Principle

Koji Kudo<sup>1,2,\*</sup>, Yoshihito Kuno<sup>1,†</sup> and Yasuhiro Hatsugai<sup>1,2</sup>

<sup>1</sup>*Department of Physics, University of Tsukuba, Tsukuba, Ibaraki 305-8571, Japan*

<sup>2</sup>*Graduate School of Pure and Applied Sciences, University of Tsukuba, Tsukuba, Ibaraki 305-8571, Japan*

(Dated: January 21, 2022)

Using the Laughlin's argument on a torus with two pin-holes, we numerically demonstrate that the discontinuities of the center-of-mass work well as an invariant of the pumping phenomena during the process of the flux-attachment, trading the magnetic flux for the statistical one. This is consistent with the bulk-edge correspondence of the fractional quantum Hall effect of anyons. We also confirm that the general feature of the edge states remains unchanged during the process while the topological degeneracy is discretely changed. This supports the stability of the quantum Hall edge states in the adiabatic heuristic principle.

**Introduction** — Characterization of quantum matter with topological invariants is a modern notion in condensed matter physics [1–4]. The adiabatic deformation of gapped systems is a conceptual basis in the theory of topological phases beyond the Landau's symmetry breaking paradigm [5, 6]. Meanwhile, augmented by the symmetry, this notion leads to more unified picture exemplified by the “periodic table” for topologically nontrivial states [7–10] and demonstrates the existence of rich topological phases. The adiabatic deformation also gives a useful way to characterize concrete models by reducing them to simple systems [11–17].

The adiabatic heuristic argument of the quantum Hall (QH) effect [11–13] is the historical example in which the adiabatic deformation has been successfully used. The fractional QH (FQH) effect [18, 19] is a topological ordered phase [20] with fractionalized excitations [21–23]. Even though it is intrinsically a many-body problem of correlated electrons unlike the integer QH (IQH) effect [1, 24–26], the composite fermion theory [27, 28] gives a unified scheme to describe their underlying physics: the FQH state at the filling factor  $\nu = p/(2mp \pm 1)$  with  $p, m$  integers can be interpreted as the  $\nu = p$  IQH state of the composite fermions. By continuously trading the external flux for the statistical one [29, 30], both states are adiabatically connected through intermediate systems of anyons (adiabatic heuristic principle [11–13]). Even though the ground state degeneracy [31, 32] is wildly changed in the periodic geometry [12, 33], the energy gap remains open and its many-body Chern number [34] works well as an adiabatic invariant [33].

Generally bulk topological invariants such as the Chern number are intimately related to the presence of gapless edge excitations. This is the so-called bulk-edge correspondence [35–37], which is a universal feature of topological phases [3, 4, 38–46]. The edges of the QH systems demonstrate the nontrivial transport properties enriched by the bulk topology, which has attracted a great interest for over decades [20, 25, 26, 35, 47–67]. The main goal in this work is to reveal how the quantum Hall edge states are evolved during the process of the flux-attachment in the adiabatic heuristic principle.

In this Letter, we analyze the fractional pumping phenomena associated with the Laughlin's argument of the anyonic FQH effect. We show that the general feature of the energy spectrum with edges shows little change during the process of the flux-attachment while the topological degeneracy is wildly changed. Furthermore, the total jump of the center-of-mass works well as an invariant of this process, which is consistent with the bulk-edge correspondence of the FQH effect of anyons. This implies that the total jump of the center-of-mass characterizes the fractional charge pumping of the adiabatic heuristic principle. Also, this supports the stability of the QH edge states in the adiabatic heuristic principle.

**Charge pumping** — Let us consider the QH system on a square lattice with  $N_x \times N_y$  sites, where  $N_x/N_y = 2$  and the periodic boundary condition is imposed. As shown in Fig. 1(a), local fluxes  $\pm\xi$  are set at two plaquettes  $A_{\pm}$  with the same  $y$  coordinate. Their distance is  $N_x/2$ . Particles are pumped from  $A_-$  to  $A_+$  as  $\xi$  varies from 0 to 1 [see Fig. 1(b)], which we call the (fractional) charge pump [68–79] throughout this Letter.

This charge pump can be mapped into the one-

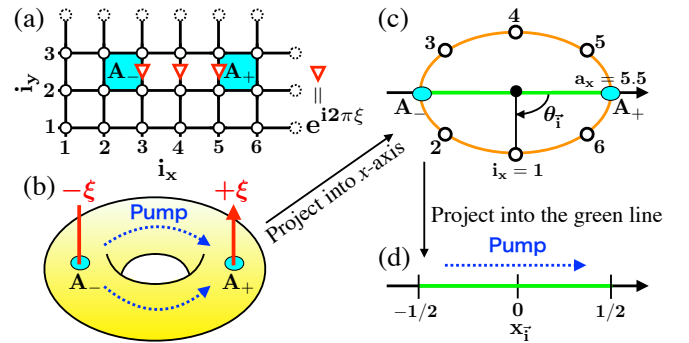


FIG. 1. (a) Sketch of  $6 \times 3$  square lattice. The gauge  $\xi_{ij}$  (red arrows) describes the two local fluxes  $\pm\xi$  at  $A_{\pm}$ . (b) Charge pump from  $A_-$  to  $A_+$ . (c) One-dimensional projection into  $x$ -axis. The projected sites for (a) are shown. The angle  $\theta_i$  is measured from  $a_x$  that is the  $x$  coordinate of  $A_+$ . (d) One-dimensional charge pump on  $-1/2 \leq x_i \leq 1/2$ .

dimensional pump with *edges* [Fig. 1(d)]. As shown in Fig. 1(c), we first project the system into the  $x$ -axis. Then, projecting it into the green line shown in Figs 1(c), we finally define a new coordinate for site  $\vec{i} = (i_x, i_y)$  as  $x_{\vec{i}} = (1/2) \cos \theta_{\vec{i}}$  with  $\theta_{\vec{i}} = 2\pi(i_x - a_x)/N_x$ , where  $a_x$  is the  $x$  coordinate of  $A_+$ , see Fig. 1(d). In this projection, the two pin-holes  $A_{\pm}$  are mapped into the edges  $x_{\vec{i}} = \pm 1/2$ .

The charge can be transformed from  $x_{\vec{i}} = -1/2$  to  $x_{\vec{i}} = 1/2$  as  $\xi$  increases. The pumped charge is given by the integration of  $\partial_{\xi} P(\xi)$ , where  $P$  is the center-of-mass,

$$P(\xi) = \text{Tr} [\rho(\xi) \sum_{\vec{i}} x_{\vec{i}} n_{\vec{i}}], \quad (1)$$

$\rho$  is the zero temperature density matrix in the grand canonical ensemble and  $n_{\vec{i}}$  is the number operator at the site  $\vec{i}$ . (In Sec. S1 of Supplemental Material [80], we derive the pumped charge by using the current operator.) As  $\xi$  varies,  $P(\xi)$  jumps several times due to the sudden change of the particle number [43, 44, 81]. Accordingly, the pumped charge between the period  $\xi \in [0, 1]$  is given by  $Q = \left( \int_0^{\xi_1^-} + \int_{\xi_1^+}^{\xi_2^-} + \cdots + \int_{\xi_N^+}^1 \right) d\xi \partial_{\xi} P(\xi)$ , where  $\xi_1, \dots, \xi_N$  are the jumping points in the period and  $\xi_{\alpha}^{\pm} = \xi_{\alpha} \pm 0$ . Using the periodicity  $P(1) = P(0)$  and  $\Delta P(\xi_{\alpha}) \equiv P(\xi_{\alpha}^+) - P(\xi_{\alpha}^-)$ , we get [43]

$$Q = - \sum_{\alpha=1}^N \Delta P(\xi_{\alpha}) \equiv -\Delta P_{\text{tot}}. \quad (2)$$

As shown below, the total jump  $\Delta P_{\text{tot}}$ , i.e., the sudden changes of the particle number, comes from the (dis)appearance of edge states. Equation (2) implies that the pumped charge is given only by the information of edges.

*Bulk-edge correspondence* — In this Letter, we numerically show the following bulk-edge correspondence for the FQH states of anyons:

$$C = -N_D \times \Delta P_{\text{tot}}, \quad (3)$$

where  $C$  is the many-body Chern number [34] of the  $N_D$ -fold degenerate ground state multiplet at  $\xi = 0$ . This is consistent with the Laughlin's argument applied to the FQH systems [1, 25, 26, 34, 36, 43, 68, 76, 82–84] that implies  $Q = C/N_D$ . In the following, we clarify how the fractional charge pumping is deformed to the standard pumping phenomena by the flux-attachment transformation. As mentioned below, the relation in Eq. (3) results in the stability of the QH edge states in the adiabatic heuristic principle.

*Fermion pumping* — As a first step, we confirm Eq. (3) for the IQH system of non-interacting fermions. The Hamiltonian is  $H = -t \sum_{\langle ij \rangle} e^{i\phi_{ij}} e^{i\xi_{ij}} c_i^{\dagger} c_j$ , where  $c_i^{\dagger}$  is the creation operator for a fermion on site  $i$  and  $t = 1$ . The phase factors  $e^{i\phi_{ij}}$  and  $e^{i\xi_{ij}}$  describe the

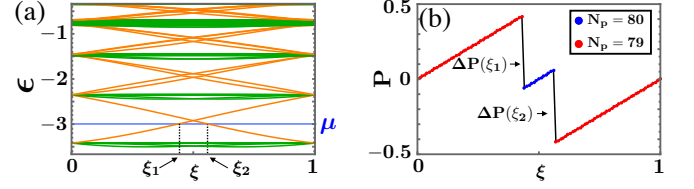


FIG. 2. (a) Single-particle energy  $\epsilon$  on  $40 \times 20$  lattices with  $\phi = 1/10$ . The green (orange) plots represent the bulk (edge) states. The blue line is  $\mu = -3$ . (b) Center-of-mass  $P$ . The two jumps are  $\Delta P(\xi_1) \approx \Delta P(\xi_2) \approx -0.48$ .

uniform magnetic field [85, 86] and the local fluxes at  $A_{\pm}$  [see Fig. 1(a)], respectively. We plot in Fig. 2(a) the single-particle energy  $\epsilon$  with  $N_x \times N_y = 40 \times 20$  and  $\phi \equiv N_{\phi}/(N_x N_y) = 1/10$ , where  $N_{\phi}$  is the total uniform fluxes. Each set of  $N_{\phi} (= 80)$  states forms the Landau level (LL) at  $\xi = 0$ . As  $\xi$  increases, some edge states go over to the mid-gap region. In Fig. 2(b), we compute  $P(\xi)$  with  $\rho = |G\rangle\langle G|$  in Eq. (1), where  $|G\rangle$  is the ground state completely occupying the 1st LL under the chemical potential (Fermi energy)  $\mu = -3$ . The sudden change of the particle number  $N_p$  causes the jumps of  $P(\xi)$  at  $\xi_1$  and  $\xi_2$ . Both values of  $\Delta P(\xi_{\alpha})$ 's are approximately  $-1/2$ , which is consistent with Fig. 2(a) where one edge state at  $x_{\vec{i}} = 1/2$  goes over across  $\mu$  and then another at  $x_{\vec{i}} = -1/2$  goes back. Although a finite size effect gives  $\Delta P_{\text{tot}} = \Delta P(\xi_1) + \Delta P(\xi_2) \approx -0.96$ , we confirm  $\Delta P_{\text{tot}} = -1$  in the thermodynamic limit (see Sec. S2 of Supplemental Material [80]). This is consistent with Eq. (3) with  $N_D = 1$  and  $C = 1$ . The cases for  $C = 2$  and 3 have been also confirmed.

*Normalized jumps* — As mentioned above, the jump  $\Delta P(\xi_{\alpha})$  are not quantized to  $\pm 1/2$  due to the finite size effect. Let us then properly normalize each jumps: when  $P$  jumps positively or negatively at  $\xi_{\alpha}$ , we assign it as  $\Delta P(\xi_{\alpha}) \mapsto 1/2$  or  $-1/2$ . Hereafter “ $\mapsto$ ” denotes this normalization; e.g., we have  $\Delta P_{\text{tot}} = P(\xi_1) + P(\xi_2) \mapsto -1/2 - 1/2 = -1$  in Fig. 2(b). This gives the bulk-edge correspondence in Eq. (3) even for finite systems.

*Fractional anyon pumping* — Let us consider the fractional pumping of anyons. To this end, we take the Hamiltonian as  $H = -t \sum_{\langle ij \rangle} e^{i\phi_{ij}} e^{i\xi_{ij}} e^{i\theta_{ij}} c_i^{\dagger} c_j$ , where the phase factor  $\theta_{ij}$  [87–89] depends on the configuration of all particles  $\{\mathbf{r}_k\}_{1 \leq k \leq N_p}$ , which describes the fractional statistics  $e^{i\theta}$ . Note that although  $c_i^{\dagger}$  is the creation operator for a fermion,  $H$  is the Hamiltonian of anyons and includes intrinsically the many-body interactions. Due to constraints of the braid group,  $\dim H$  depends on  $\theta$  even for the same  $N_p$  [87, 90]: the Hilbert space for  $\theta/\pi = n/m$  ( $n, m$ : coprime) is spanned by the basis  $|\{\mathbf{r}_k\}; w\rangle$ , where  $w = 1, \dots, m$  is an additional internal degree of freedom. When a particle hops across the boundary in the  $x$  direction, the label is shifted from  $w$  to  $w - 1$ . As for

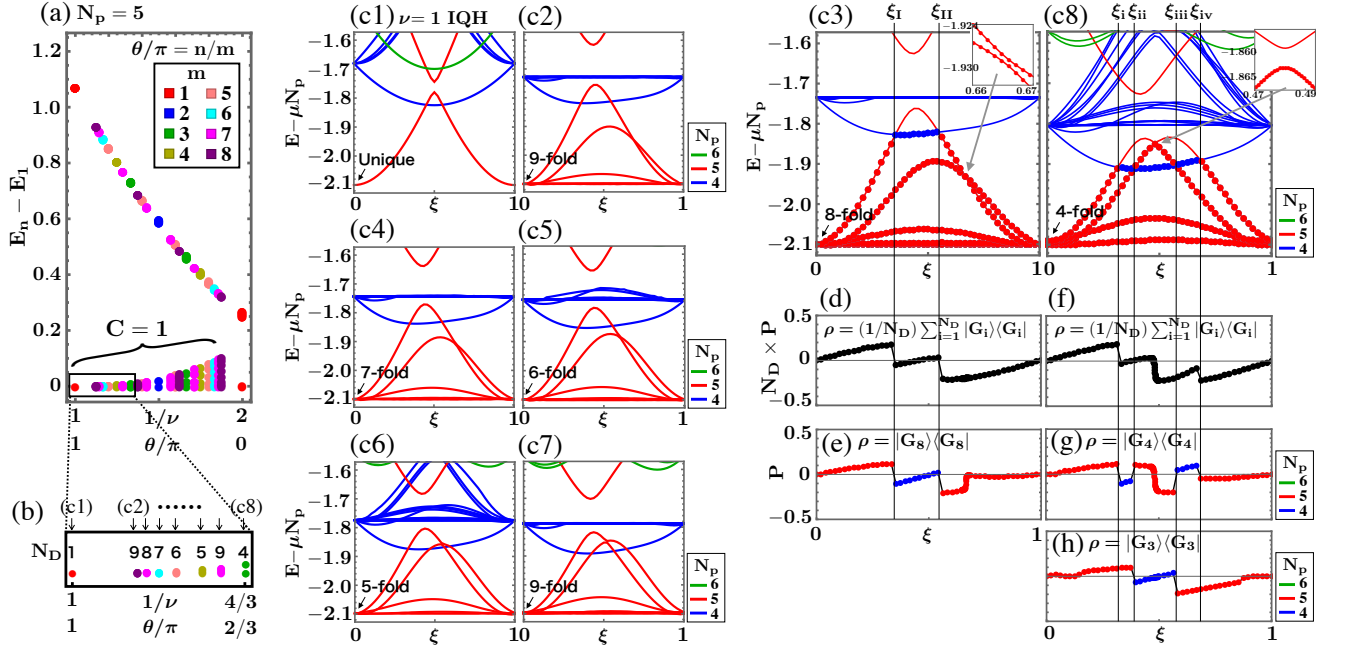


FIG. 3. (a) Energy gaps as functions of  $1/\nu$  at  $\xi = 0$  with  $N_p = 5$ . The statistical angle  $\theta$  is determined by  $\nu = p/[p(1-\theta/\pi)+1]$  with  $p = 1$ . The color expresses the denominator of  $\theta/\pi$ . (b) Ground state degeneracy  $N_D$ . (c1)-(c8) Energy spectra as functions of local fluxes  $\xi$ . Each value of  $(\nu, \theta)$  is represented above the panel (b). We set  $\mu = -3$  in (c1) and choose  $\mu$  in (c2)-(c8) so that the lowest energy at  $\xi = 0$  is same as that in (c1). In (c3) and (c8), the  $N_D$  lowest energy states are marked by dots. In (a)-(c), we plot the lowest  $N_{\text{cut}}$  energies with  $N_{\text{cut}} = 2$  for  $N_p = 6$  and  $N_{\text{cut}} = 20$  for  $N_p = 5, 4$ . (d)-(h) Center of mass  $P$  as for the panels (c3) and (c8).  $\xi_I, \xi_{II}$  and  $\xi_i - \xi_{iv}$  represent the gap closing points.

the boundary in the  $y$  direction, the phase factor  $e^{iw\theta}$  is given. Thanks to this, global requirements of anyons hold [87, 88, 90, 91]. Also, we introduce  $\xi_{ij}$  only for the basis with  $w = 1$  [92].

In the following, we focus on a family of the  $\nu = 1$  IQH states connected by trading the magnetic fluxes for statistical ones [11, 12, 27, 33]:  $\nu = p/[p(1-\theta/\pi)+1]$  with  $p = 1$ . Fixing  $N_x \times N_y = 10 \times 5$ ,  $N_p = 5$  and  $\xi = 0$ , we plot the energy gaps as functions of  $1/\nu$  in Fig. 3(a). Due to the lattice, the topological degeneracy is lifted. We here define the low-energy states with  $E_n - E_1 < 0.2$  as the ground state multiplet. The ground state at  $\nu = s/t$  ( $s, t$ : coprime) in Fig. 3(a) gives the degeneracy  $N_D = t$  numerically [see Fig. 3(b)] and the Chern numbers of the multiplets are always  $C = 1$  [33]. Namely, the many-body Chern number is used as an adiabatic invariant. The gap closing at  $\nu \approx 1/2$  is expected due to finite-size effects [33].

Let us investigate the pumping phenomena. As for each parameter  $(1/\nu, \theta/\pi)$  shown in Fig. 3(b), we plot in Figs. 3(c1)-(c8) the eigenvalues of the Hamiltonian including the chemical potential,  $H - \mu N_p$ , as functions of  $\xi$  with  $4 \leq N_p \leq 6$  [93]. Figure 3(c1) is in the same setting of Fig. 2 but for smaller system sizes. In Fig 3(c1), the particle number  $N_p$  of the unique ground state is changed as  $\xi$  increases due to the (dis)appearance of the edge state as mentioned previously. The gap between the

two red lines at  $\xi \approx 0.5$  is a finite-size effect. As shown in Figs. 3(c1)-(c8), even though the topological degeneracy is wildly changed as  $1/\nu$  and  $\theta/\pi$  vary, the general feature of the spectra remains unchanged. The degenerate ground states at  $\xi = 0$  are lifted as  $\xi$  increases and then one or two states float up in energy to cross with another state having one particle less.

Now we focus on the anyonic system in Fig. 3(c3) and show its the bulk-edge correspondence. Here  $\theta/\pi = 6/7$ ,  $\nu = 7/8$  and  $N_D = 8$  at  $\xi = 0$ . To define the center-of-mass of the ground state multiplet suitably, we define the density matrix as  $\rho(\xi) = (1/N_D) \sum_{k=1}^{N_D} |G_k(\xi)\rangle \langle G_k(\xi)|$ , where  $|G_k(\xi)\rangle$  is the  $k$ -th lowest energy state. Using it with Eq. (1), we plot  $N_D \times P(\xi)$  in Fig. 3(d). There are two jumps at  $\xi_I$  and  $\xi_{II}$ , where the  $N_D$ th and  $N_D + 1$ th lowest energy states cross each other in the spectrum. Because of  $N_D \rho = \sum_{k=1}^{N_D} |G_k\rangle \langle G_k|$ , the obtained jumps are solely given by  $P$  with  $\rho = |G_{N_D}\rangle \langle G_{N_D}|$  shown in Fig. 3(e). This figure gives  $\Delta P_{\text{tot}} = \Delta P(\xi_I) + P(\xi_{II}) \mapsto -1$ , which implies  $N_D \times \Delta P_{\text{tot}} \mapsto -1$  in Fig. 3(d). This is consistent with Eq. (3) with  $C = 1$ . Because of  $Q = -\Delta P_{\text{tot}}$ , we have the fractional pumped charge  $Q = 1/8$ . In this argument, we assume the absence of the gap closing between states with the same  $N_p$  apart from  $\xi = 0$  since there are no symmetry except for the charge  $U(1)$ . The gap at  $\xi \approx 0.7$  between  $|G_{N_D}\rangle$  and  $|G_{N_D-1}\rangle$  is very small but is finite [94] as shown in the

inset.

Let us here mention the finite size effect in Fig. 3(d). The value of  $N_D \times \Delta P_{\text{tot}}$  before normalizing is about  $-0.46$ , which is far away from  $-1$ . Although this value in the IQH system in Fig. 3(c1) is about the same magnitude (about  $-0.60$ , see the data point at  $\nu = 1$  of Fig. 4), it approaches  $-1$  as the system size increases as confirmed in Sec. S2 of Supplemental Material [80]. Since the bulk gaps of the two systems are comparable and their system sizes are same, the deviation from  $-1$  in Fig. 3(d) is also expected to be the finite size effect.

Let us next focus on the system in Fig. 3(c8), where  $\theta/\pi = 2/3$ ,  $\nu = 3/4$  and  $N_D = 4$  at  $\xi = 0$ . Unlike the previous case, there are four gap-closing points,  $\xi_i \cdots \xi_{iv}$ , as for the  $N_D$  lowest energy states. However,  $P(\xi)$  with  $\rho = (1/N_D) \sum_{k=1}^{N_D} |G_k\rangle\langle G_k|$  in Fig. 3(f) jumps only at  $\xi_i$  and  $\xi_{iv}$  because the jumps at  $\xi_{ii}, \xi_{iii}$  cancel each other, see Figs. 3(g) and 3(h). Consequently, the total jump is given by  $N_D \times \Delta P_{\text{tot}} \mapsto -1$ , which is consistent with Eq. (3) with  $C = 1$ . This implies the fractional pumped charge  $Q = 1/4$ . The gap at  $\xi \approx 0.5$  is very small but is finite as mentioned before, see the inset in Fig. 3(c8).

The results shown in Figs. 3(c3) and 3(c8) suggest that  $N_D \times \Delta P_{\text{tot}}$  is the invariant of the bulk gap in the process of the flux-attachment. To demonstrate it, we plot the total jumps as functions of  $1/\nu$  in Fig. 4, where both data before/after normalizing each jumps are shown. The normalized data justify that  $N_D \times \Delta P_{\text{tot}}$  works well as the invariant. This nature is also indicated by the unnormalized data in Fig. 4: the plots are *smooth* as  $1/\nu$  and  $\theta/\pi$  vary even though (i) the degeneracy  $N_D$  is *wildly* changed and (ii) the dimension of the Hamiltonian is *discretely* changed depending on the denominator of  $\theta/\pi$ : e.g., with  $N_p = 5$ ,  $\dim H = \binom{N_x N_y}{N_p} = \binom{50}{5} = 2118760$  for  $\theta/\pi = n$  while  $\dim H = 11 \binom{50}{5} = 23306360$  for  $\theta/\pi = n/11$  (this is due to the additional internal degree  $w$  of the basis  $|\{\mathbf{r}_k\}; w\rangle$  as mentioned above). We stress that this non-trivial smoothness in Fig. 4 implies the stability of the QH edge states in the adiabatic heuristic principle.

**Conclusion** — In this Letter, we demonstrate the bulk-edge correspondence of the FQH states of anyons. The results indicate that the total jump of the center-of-mass, which corresponds to the many-body Chern number, is an invariant with respect to the flux-attachment. This implies the stability of edge states in the adiabatic heuristic principle. Recently, direct observation of the center of mass in pumping phenomena has been conducted in cold atoms [70, 71]. The behavior of the center-of-mass that we focus on would be observed in cold atoms although the experimental realization of the two-dimensional anionic system is still a challenging problem.

We thank the Supercomputer Center, the Institute for Solid State Physics, the University of Tokyo for the use of the facilities. The work is supported in part by JSPS KAKENHI Grant Numbers JP17H06138, JP19J12317

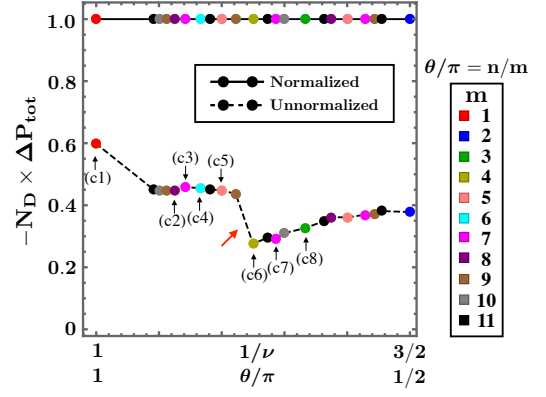


FIG. 4. The total jump of the center-of-mass  $N_D \times \Delta P_{\text{tot}}$ . The solid and dotted lines mean the normalized and the unnormalized data, respectively. The systems in Figs. 3(c1)-(c8) are marked. The sudden change in the dotted line, represented by a red arrow, is due to the gap collapse of the  $N_D - 1$ th lowest energy state, compare Figs. 3(c5) and 3(c6). The jumps are calculated by discretizing the period  $\xi \in [0, 1]$  into  $N_\xi$  meshes with  $N_\xi = 48$  (Only at (c6) point, we set  $N_\xi = 240$ ).

(K.K.), and JP21K13849 (Y.K.).

\* Present address: Department of Physics, 104 Davey Lab, The Pennsylvania State University, University Park, Pennsylvania 16802, USA

† Present address: Graduate School of Engineering Science, Akita University, Akita, 010-8502, Japan

- [1] D. J. Thouless, M. Kohmoto, M. P. Nightingale, and M. den Nijs, Phys. Rev. Lett. **49**, 405 (1982).
- [2] M. Kohmoto, Annals of Physics **160**, 343 (1985).
- [3] M. Z. Hasan and C. L. Kane, Rev. Mod. Phys. **82**, 3045 (2010).
- [4] X.-L. Qi and S.-C. Zhang, Rev. Mod. Phys. **83**, 1057 (2011).
- [5] X. G. Wen, Phys. Rev. B **40**, 7387 (1989).
- [6] X.-G. Wen, Rev. Mod. Phys. **89**, 041004 (2017).
- [7] A. Kitaev, AIP Conference Proceedings **1134**, 22 (2009).
- [8] A. P. Schnyder, S. Ryu, A. Furusaki, and A. W. W. Ludwig, Phys. Rev. B **78**, 195125 (2008).
- [9] X.-L. Qi, T. L. Hughes, and S.-C. Zhang, Phys. Rev. B **78**, 195424 (2008).
- [10] S. Ryu, A. P. Schnyder, A. Furusaki, and A. W. W. Ludwig, New Journal of Physics **12**, 065010 (2010).
- [11] M. Greiter and F. Wilczek, Modern Physics Letters B **04**, 1063 (1990).
- [12] M. Greiter and F. Wilczek, Nuclear Physics B **370**, 577 (1992).
- [13] M. Greiter and F. Wilczek, (2021), arXiv:2105.05625 [cond-mat.mes-hall].
- [14] Y. Hatsugai, Journal of the Physical Society of Japan **74**, 1374 (2005).
- [15] Y. Hatsugai, Journal of the Physical Society of Japan **75**, 123601 (2006).



- [16] Y. Hatsugai, *Journal of Physics: Condensed Matter* **19**, 145209 (2007).
- [17] T. Kariyado, T. Morimoto, and Y. Hatsugai, *Phys. Rev. Lett.* **120**, 247202 (2018).
- [18] D. C. Tsui, H. L. Stormer, and A. C. Gossard, *Phys. Rev. Lett.* **48**, 1559 (1982).
- [19] R. B. Laughlin, *Phys. Rev. Lett.* **50**, 1395 (1983).
- [20] X.-G. Wen, *Advances in Physics* **44**, 405 (1995).
- [21] F. D. M. Haldane, *Phys. Rev. Lett.* **51**, 605 (1983).
- [22] B. I. Halperin, *Phys. Rev. Lett.* **52**, 1583 (1984).
- [23] D. Arovas, J. R. Schrieffer, and F. Wilczek, *Phys. Rev. Lett.* **53**, 722 (1984).
- [24] K. v. Klitzing, G. Dorda, and M. Pepper, *Phys. Rev. Lett.* **45**, 494 (1980).
- [25] R. B. Laughlin, *Phys. Rev. B* **23**, 5632 (1981).
- [26] B. I. Halperin, *Phys. Rev. B* **25**, 2185 (1982).
- [27] J. K. Jain, *Phys. Rev. Lett.* **63**, 199 (1989).
- [28] J. K. Jain, *Composite Fermions* (Cambridge University Press, 2007).
- [29] F. Wilczek, *Phys. Rev. Lett.* **48**, 1144 (1982).
- [30] F. Wilczek, *Phys. Rev. Lett.* **49**, 957 (1982).
- [31] F. D. M. Haldane, *Phys. Rev. Lett.* **55**, 2095 (1985).
- [32] X. G. Wen and Q. Niu, *Phys. Rev. B* **41**, 9377 (1990).
- [33] K. Kudo and Y. Hatsugai, *Phys. Rev. B* **102**, 125108 (2020).
- [34] Q. Niu, D. J. Thouless, and Y.-S. Wu, *Phys. Rev. B* **31**, 3372 (1985).
- [35] X. G. Wen, *Phys. Rev. Lett.* **64**, 2206 (1990).
- [36] Y. Hatsugai, *Phys. Rev. Lett.* **71**, 3697 (1993).
- [37] Y. Hatsugai, *Phys. Rev. B* **48**, 11851 (1993).
- [38] C. L. Kane and E. J. Mele, *Phys. Rev. Lett.* **95**, 226801 (2005).
- [39] F. D. M. Haldane and S. Raghu, *Phys. Rev. Lett.* **100**, 013904 (2008).
- [40] T. Kariyado and Y. Hatsugai, *Scientific Reports* **5**, 18107 (2015).
- [41] P. Delplace, J. B. Marston, and A. Venaille, *Science* **358**, 1075 (2017).
- [42] K. Sone and Y. Ashida, *Phys. Rev. Lett.* **123**, 205502 (2019).
- [43] Y. Hatsugai and T. Fukui, *Phys. Rev. B* **94**, 041102 (2016).
- [44] Y. Kuno and Y. Hatsugai, *Phys. Rev. Research* **2**, 042024 (2020).
- [45] T. Mizoguchi, T. Yoshida, and Y. Hatsugai, *Phys. Rev. B* **103**, 045136 (2021).
- [46] T. Yoshida, T. Mizoguchi, and Y. Hatsugai, (2020), arXiv:2012.05562 [cond-mat.mes-hall].
- [47] A. H. MacDonald, *Phys. Rev. Lett.* **64**, 220 (1990).
- [48] X. G. Wen, *Phys. Rev. B* **41**, 12838 (1990).
- [49] X. G. Wen, *Phys. Rev. B* **43**, 11025 (1991).
- [50] M. D. Johnson and A. H. MacDonald, *Phys. Rev. Lett.* **67**, 2060 (1991).
- [51] X.-G. Wen, *International Journal of Modern Physics B* **06**, 1711 (1992).
- [52] C. d. C. Chamon and X. G. Wen, *Phys. Rev. B* **49**, 8227 (1994).
- [53] Y. Meir, *Phys. Rev. Lett.* **72**, 2624 (1994).
- [54] C. L. Kane, M. P. A. Fisher, and J. Polchinski, *Phys. Rev. Lett.* **72**, 4129 (1994).
- [55] C. L. Kane and M. P. A. Fisher, *Phys. Rev. B* **51**, 13449 (1995).
- [56] X. Wan, K. Yang, and E. H. Rezayi, *Phys. Rev. Lett.* **88**, 056802 (2002).
- [57] Y. N. Joglekar, H. K. Nguyen, and G. Murthy, *Phys. Rev. B* **68**, 035332 (2003).
- [58] X. Wan, E. H. Rezayi, and K. Yang, *Phys. Rev. B* **68**, 125307 (2003).
- [59] A. M. Chang, *Rev. Mod. Phys.* **75**, 1449 (2003).
- [60] Z.-X. Hu, H. Chen, K. Yang, E. H. Rezayi, and X. Wan, *Phys. Rev. B* **78**, 235315 (2008).
- [61] Z.-X. Hu, E. H. Rezayi, X. Wan, and K. Yang, *Phys. Rev. B* **80**, 235330 (2009).
- [62] J. Wang, Y. Meir, and Y. Gefen, *Phys. Rev. Lett.* **111**, 246803 (2013).
- [63] C. Repellin, A. M. Cook, T. Neupert, and N. Regnault, *npj Quantum Materials* **3**, 14 (2018).
- [64] R. Fern, R. Bondesan, and S. H. Simon, *Phys. Rev. B* **98**, 155321 (2018).
- [65] L.-X. Wei, N. Jiang, Q. Li, and Z.-X. Hu, *Phys. Rev. B* **101**, 075137 (2020).
- [66] T. Ito and N. Shibata, *Phys. Rev. B* **103**, 115107 (2021).
- [67] U. Khanna, M. Goldstein, and Y. Gefen, *Phys. Rev. B* **103**, L121302 (2021).
- [68] D. J. Thouless, *Phys. Rev. B* **27**, 6083 (1983).
- [69] L. Wang, M. Troyer, and X. Dai, *Phys. Rev. Lett.* **111**, 026802 (2013).
- [70] S. Nakajima, T. Tomita, S. Taie, T. Ichinose, H. Ozawa, L. Wang, M. Troyer, and Y. Takahashi, *Nature Physics* **12**, 296 (2016).
- [71] M. Lohse, C. Schweizer, O. Zilberberg, M. Aidelsburger, and I. Bloch, *Nature Physics* **12**, 350 (2016).
- [72] H. Guo, S.-Q. Shen, and S. Feng, *Phys. Rev. B* **86**, 085124 (2012).
- [73] Z. Xu, L. Li, and S. Chen, *Phys. Rev. Lett.* **110**, 215301 (2013).
- [74] T.-S. Zeng, C. Wang, and H. Zhai, *Phys. Rev. Lett.* **115**, 095302 (2015).
- [75] H. Hu, H. Guo, and S. Chen, *Phys. Rev. B* **93**, 155133 (2016).
- [76] T.-S. Zeng, W. Zhu, and D. N. Sheng, *Phys. Rev. B* **94**, 235139 (2016).
- [77] M. Nakagawa and S. Furukawa, *Phys. Rev. B* **95**, 165116 (2017).
- [78] L. Taddia, E. Cornfeld, D. Rossini, L. Mazza, E. Sela, and R. Fazio, *Phys. Rev. Lett.* **118**, 230402 (2017).
- [79] M. Nakagawa, T. Yoshida, R. Peters, and N. Kawakami, *Phys. Rev. B* **98**, 115147 (2018).
- [80] See Supplemental Material at <http://...>, for details of the relation between the pumped charge and the current operator, and a finite size scaling analysis, which includes Ref. 95.
- [81] Y. Kuno and Y. Hatsugai, *Phys. Rev. B* **104**, 045113 (2021).
- [82] D. J. Thouless, *Phys. Rev. B* **40**, 12034 (1989).
- [83] A. G. Grushin, J. Motruk, M. P. Zaletel, and F. Pollmann, *Phys. Rev. B* **91**, 035136 (2015).
- [84] B. Andrews, M. Mohan, and T. Neupert, *Phys. Rev. B* **103**, 075132 (2021).
- [85] D. R. Hofstadter, *Phys. Rev. B* **14**, 2239 (1976).
- [86] Y. Hatsugai, K. Ishibashi, and Y. Morita, *Phys. Rev. Lett.* **83**, 2246 (1999).
- [87] X. G. Wen, E. Dagotto, and E. Fradkin, *Phys. Rev. B* **42**, 6110 (1990).
- [88] Y. Hatsugai, M. Kohmoto, and Y.-S. Wu, *Phys. Rev. B* **43**, 10761 (1991).
- [89] The Hamiltonian is also expressed by using the creation-annihilation operators of hard-core bosons with the sta-

tistical flux. In the numerical calculations, we diagonalize it because of its technical simplicity.

- [90] T. Einarsson, Phys. Rev. Lett. **64**, 1995 (1990).
- [91] A global requirement of anyons on a torus [87, 90] is  $\rho_i^{-1} \tau_j \rho_i \tau_j^{-1} = A_{ij}$ , where  $\tau_i$  and  $\rho_i$  are global move operators of particle  $i$  along noncontractible loops on the torus in  $x$  and  $y$  directions, and  $A_{ij}(= e^{i2\theta})$  is a local move operator of particle  $i$  around particle  $j$ .
- [92] The many-body Chern number that is invariant for the adiabatic heuristic principle is given by the following twisted boundary conditions [33]: when an anyon hops across the boundary in  $x$  ( $y$ ) direction, the phase factor  $e^{i\theta_x \delta_{w,1}} (e^{i\theta_y})$  is given to the basis  $|\{\mathbf{r}_k\}; w\rangle$ . According to this rule in  $x$  direction, we define the local fluxes  $\pm\xi$  only for  $w = 1$ .
- [93] For fermions, we change  $N_p$  keeping  $N_\phi$  constant. Such a change for anyons is prohibited by constraints of the braid group [90]. Thus we change their  $N_p$  in such a way that the total flux  $N_\phi + N_p \times \theta/\pi$  is same as that in the case of fermions.
- [94] Because of the mid-gap region,  $|G_{N_D}\rangle$  and  $|G_{N_D-1}\rangle$  at  $\xi \approx 0.7$  have edge modes. It is suggested that they are localized at the opposite edges each other. Either one is expected due to finite size effects.
- [95] Y. Hatsugai, Journal of the Physical Society of Japan **73**, 2604 (2004).

## Supplemental Material

### S1. CURRENT OPERATOR AND THE PUMPED CHARGE

In this appendix, we derive the pumped charge  $Q$  by using the current operator. We consider the Hamiltonian described in the paragraph *Fractional anyon pumping* in the main text:

$$H(\xi) = -t \sum_{\langle \vec{i}, \vec{j} \rangle} e^{i\phi_{\vec{i}, \vec{j}}} e^{i\xi_{\vec{i}, \vec{j}}} e^{i\theta_{\vec{i}, \vec{j}}} c_{\vec{i}}^\dagger c_{\vec{j}}, \quad (\text{S1})$$

where  $c_{\vec{i}}^\dagger$  is the creation operator for a fermion on site  $\vec{i}$ , and the phase factors  $e^{i\phi_{\vec{i}, \vec{j}}}$ ,  $e^{i\xi_{\vec{i}, \vec{j}}}$  and  $e^{i\theta_{\vec{i}, \vec{j}}}$  describe the uniform fluxes, the local fluxes  $\pm\xi$  and the statistical phase  $\theta$ , respectively. Using a unitary operator,

$$U(\alpha) = \prod_{\vec{i}} e^{-i\alpha x_{\vec{i}} n_{\vec{i}}},$$

let us modify the Hamiltonian in Eq. (S1):

$$\begin{aligned} H(\alpha, \xi) &\equiv U(\alpha) H(\xi) U^\dagger(\alpha) \\ &= -t \sum_{\langle \vec{i}, \vec{j} \rangle} e^{-i\alpha(x_{\vec{i}} - x_{\vec{j}})} e^{i\phi_{\vec{i}, \vec{j}}} e^{i\xi_{\vec{i}, \vec{j}}} e^{i\theta_{\vec{i}, \vec{j}}} c_{\vec{i}}^\dagger c_{\vec{j}}, \end{aligned} \quad (\text{S2})$$

where  $U(\alpha) c_{\vec{i}}^\dagger U^\dagger(\alpha) = e^{i\alpha x_{\vec{i}}} c_{\vec{i}}^\dagger$  is used. We then define the current operator in the  $x$  direction as

$$\begin{aligned} \mathcal{I}_x &= i \frac{t}{\hbar} \sum_{\langle \vec{i}, \vec{j} \rangle} (x_{\vec{i}} - x_{\vec{j}}) e^{-i\alpha(x_{\vec{i}} - x_{\vec{j}})} e^{i\phi_{\vec{i}, \vec{j}}} e^{i\xi_{\vec{i}, \vec{j}}} e^{i\theta_{\vec{i}, \vec{j}}} c_{\vec{i}}^\dagger c_{\vec{j}} \\ &= \frac{1}{\hbar} \partial_\alpha H(\alpha, \xi). \end{aligned}$$

We now assume the following density matrix:

$$\rho(\alpha, \xi) = \frac{1}{N_D} \Phi(\alpha, \xi) \Phi^\dagger(\alpha, \xi),$$

where  $\Phi(\alpha, \xi) = (|G_1(\alpha, \xi)\rangle, \dots, |G_{N_D}(\alpha, \xi)\rangle)$  is the ground state multiplet of the Hamiltonian  $H(\alpha, \xi)$ . The measured current  $I_x$  computed from  $\mathcal{I}_x$  is reduced to the Berry curvature [43, 68]:

$$\begin{aligned} I_x(\alpha, \xi) &= -\frac{i}{N_D} B(\alpha, \xi), \\ B(\alpha, \xi) &= \partial_\alpha A_\xi(\alpha, \xi) - \partial_\xi A_\alpha(\alpha, \xi), \\ A_s(\alpha, \xi) &= \text{tr} [\Phi^\dagger(\alpha, \xi) \partial_s \Phi(\alpha, \xi)], \quad s = \alpha, \xi, \end{aligned}$$

where “tr” indicates the trace of a  $N_D$ -dimensional matrix. The gauge transformation in Eq. (S2) implies

$$\Phi(\alpha, \xi) = U(\alpha) \Phi(\xi), \text{ i.e.,}$$

$$\begin{aligned} A_\alpha(\alpha, \xi) &= -\text{tr} \left[ \Phi(\xi)^\dagger \left( \sum_{\vec{i}} i x_{\vec{i}} n_{\vec{i}} \right) \Phi(\xi) \right] = i N_D P(\xi), \\ A_\xi(\alpha, \xi) &= \text{tr} [\Phi(\xi)^\dagger \partial_\xi \Phi(\xi)] \equiv A_\xi(\xi), \end{aligned}$$

where  $P(\xi)$  is the center-of-mass defined in Eq. (1). By fixing the gauge  $\Phi(\xi)$  properly [43, 68, 95], one can prepare  $A_\xi(\xi)$  as a well-defined function. Because of  $\partial_\alpha A_\xi(\xi) = 0$ , we have  $B(\alpha, \xi) = i N_D \partial_\xi P(\xi)$ , namely,

$$I_x(\alpha, \xi) = \partial_\xi P(\xi). \quad (\text{S3})$$

The pumped charge  $Q$  is given by the integration of the current  $I_x(\alpha, \xi)$  over  $\xi$ . This clearly justifies the formulation using  $P(\xi)$  in the main text.

### S2. FINITE SIZE EFFECT

Let us discuss a finite size effect of numerical simulation. In Fig. S1, we plot the total jump  $\Delta P_{\text{tot}}$  at  $\nu = 1$ , where we fix the aspect ratio, the chemical potential, and flux per plaquette as  $N_x/N_y = 2$ ,  $\mu = -3$ , and  $\phi = 1/10$ , respectively. As indicated in the figure, the systems in Figs. 2, 3(c1) and 4 are included. As the system size  $N_x$  increases,  $\Delta P_{\text{tot}}$  approaches -1. This implies that the edge modes are somewhat spread over in a finite size system, which results in the deviation from -1 at  $\nu = 1$  in Figs. 2 and 4.

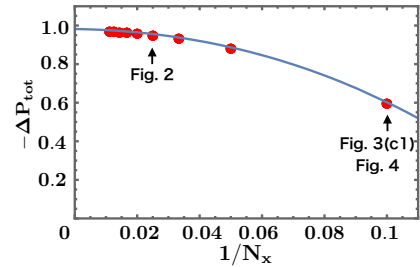


FIG. S1. Finite-size scaling analysis of the total jump  $\Delta P_{\text{tot}}$  at  $\nu = 1$ . The parameters are fixed as  $N_x/N_y = 2$ ,  $\mu = -3$ , and  $\phi = 1/10$ . Toward  $N_x \rightarrow \infty$ , the data extrapolate to  $\Delta P_{\text{tot}} = -0.98$ .